Annu. Rev. Mater. Res. 2001. 31:323–55

BLOCK COPOLYMER THIN FILMS: Physics and Applications[1]

Michael J Fasolka
Optical Technology Division, National Institute of Standards and Technology, Gaithersburg, Maryland 20899; e-mail: mfasolka@nist.gov

Anne M Mayes
Department of Materials Science and Engineering, Massachusetts Institute of Technology, Cambridge, Massachusetts 02139; e-mail: amayes@mit.edu

Key Words confinement, self-consistent field, wetting, nanoarray, nanopattern, self-assembly

■ **Abstract** A two-part review of research concerning block copolymer thin films is presented. The first section summarizes experimental and theoretical studies of the fundamental physics of these systems, concentrating upon the forces that govern film morphology. The role of film thickness and surface energetics on the morphology of compositionally symmetric, amorphous diblock copolymer films is emphasized, including considerations of boundary condition symmetry, so-called hybrid structures, and surface chemical expression. Discussions of compositionally asymmetric systems and emerging research areas, e.g., liquid-crystalline and A-B-C triblock systems, are also included. In the second section, technological applications of block copolymer films, e.g., as lithographic masks and photonic materials, are considered. Particular attention is paid to means by which microphase domain order and orientation can be controlled, including exploitation of thickness and surface effects, the application of external fields, and the use of patterned substrates.

INTRODUCTION AND SCOPE

Block copolymers (BCs) consist of two or more chemically distinct polymer fragments, or blocks, covalently bonded together to form a larger, more complex macromolecule. If the constituent polymers are immiscible, phase separation is induced on a scale that is directly related to the size of the copolymer chains, which results in morphologies typified by a pattern of chemically distinct domains of periodicity L_0 in the 10–100 nm range (1, 2). The order/disorder transition (ODT)

[1]The US Government has the right to retain a nonexclusive, royalty-free license in and to any copyright covering this paper.

temperature and the specific pattern motifs formed by a given BC are functions of the polymer molecular weight, the segmental interactions, and the volumetric composition (1, 2). The BC composition in particular strongly determines the microphase morphology. For example, diblock copolymers having blocks of comparable volume exhibit a lamellar motif. Increasing the degree of compositional asymmetry leads to the gyroid, cylindrical, and finally, spherical phases (2).

BC microphase separation has been the focus of intense research activity—both fundamental and applied—spanning the last 30 years. These efforts have produced a solid foundation of theoretical and experimental understanding of the rich behavior of these systems and provided insight into how this spontaneous nanoscopic pattern formation might be harnessed for use in a variety of technological schemes. While the majority of this work has concentrated upon bulk systems, more recent efforts have striven to understand BC microphase separation in thin films. This latter research has, in large part, been concerned with the understanding and exploitation of the enhanced role of surface/interfacial energetics, as well as the interplay between the copolymer's characteristic length scale, L_0, and the film thickness, t, in dictating film structure. Indeed, as film thickness decreases, these effects become increasingly consequential.

Our review of the current state of BC thin film research is organized into two sections First, the major ideas that constitute our understanding of BC thin film morphology are outlined. This encompasses a discussion of the experimental and theoretical treatments of the effects of confinement and surface energetics on microphase separation. This is followed by a review of research concentrating on the application of BC thin films to future technologies, with discussion centering largely on the control of thin film morphology.

As with all such reviews on extensively researched subjects, the scope of this article is limited by space. Accordingly, much of the following focuses on the simplest and most studied system, cast films of amorphous diblock copolymers that are compositionally symmetric. The topic of adsorbed block copolymer films—of relevance to colloidal and biomaterials applications—is not discussed here. Finally, the current discussion does not deal with BC thin film kinetics. A brief review of this subject can be found in an article by Matsen (3).

PHYSICS OF BC THIN FILM MORPHOLOGY

Bulk BC morphologies are typified by grains of ordered domains oriented randomly with respect to each other, much like the grain structure of small molecule or atomic crystals (2, 4, 5). In contrast, BC thin films are often characterized by highly oriented domains (6–8). This orientation is a direct result of surface and interfacial energy minimization, as illustrated by a film of a bulk-lamellar diblock with block segments denoted A and B bounded by surfaces 1 and 2 shown in Figure 1*a*,*b*. The overriding trend exhibited by films of thickness $t > L_0$ is full lamellae oriented parallel to the film and substrate surfaces (6) as shown in

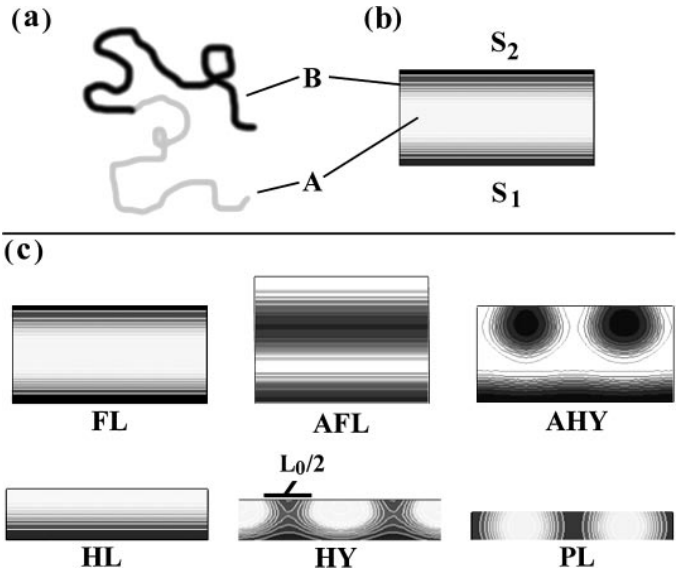

Figure 1 Diblock copolymer thin film morphologies. (*a*) Schematic representation of volume symmetric diblock with A (light) and B (dark) type segments. (*b*) Diagram of BC film system in cross section indicating the bottom (1) and top (2) surfaces, with surface interaction energies S_1 and S_2, respectively. (*c*) Summary of diblock thin film morphologies, generally organized by their appearance as film thickness decreases from L_0. These calculated cross sections indicate the density of B-type segments, i.e., Black = 100% B, white = 100% A. These structures are referred to in the text with the abbreviations included under each diagram. FL: symmetric surface-parallel full lamella; AFL: anti-symmetric surface-parallel lamella; AHY: anti-symmetric hybrid structure; HL: half-lamella; HY: symmetric hybrid structure; PL: surface-perpendicular lamellae.

Figure 1*c* (FL). This morphology develops through the surface and substrate boundary conditions that demand the most energetically compatible block be expressed at each of the surfaces. These surface-parallel lamellae also optimize the interfacial energetics of the system by minimizing the amount of A/B interface while maintaining L_0 periodicity. By convention, if the same block, for example B, is found at each boundary, the copolymer is said to exhibit symmetric wetting. Alternately, BC films that express different blocks at each surface (6, 9, 10) are termed anti-symmetric [see Figure 1*c* (AFL)]. At equilibrium, symmetric film systems exhibit a series of stable films when $t = nL_0$ ($n = 1, 2, 3, 4$), whereas anti-symmetric films exhibit a similar series of stable films when $t = (n + 1/2)L_0$.

Symmetric Boundary Energetics

The wetting and domain orientation a given BC exhibits depends upon the energetic/chemical nature of the surfaces that bound the film, i.e., the magnitude

and type of interaction (attraction/repulsion) these boundaries have with each of the block species. Surface boundary energetics can be classified into two general categories: symmetric boundary conditions, in which the energetics imposed by each surface is identical, and asymmetric boundary conditions consisting of surfaces with different energetic qualities. Research considering symmetric boundary conditions is discussed below.

THEORY Several researchers have used theoretical techniques to examine the prospect of morphological shifts as a function of film thickness for the case of lamellar diblock films bounded by identical or neutral surfaces, i.e., symmetric surface energetics. This problem was first approached by Turner (11), who used a scaling analysis to determine the relative stability of symmetric versus antisymmetric lamellae as a function of film thickness and surface potential. Walton et al (12) extended this effort to first consider the case of lamellae oriented perpendicular to the film surfaces. This lateral arrangement [or perpendicular lamellae (PL) seen in Figure 1*c*] relaxes the entropic penalty imposed on chains when surface-parallel lamellae are constrained to film thicknesses incommensurate with integer multiples of L_0. Comparing this advantage with the surface and interfacial penalties associated with lamellar reorientation, these researchers (12) outlined the following trends. First, the domain orientation was film thickness dependent. In particular, PL gained stability when $t \neq nL_0$, and especially for $t < L_0$. Second, for neutral surface energetics, PL was stable for all film thicknesses. As will be seen, this neutrality condition in surface energetics has technological implications.

Using computational approaches, other researchers have verified and expanded upon the concept of thickness-dependent domain orientation under symmetric boundary conditions (13–17). Pickett & Balazs (13) employed two-dimensional self-consistent mean-field (SCF) calculations to test the neutrality condition by comparing the equilibrium morphologies found for both neutral and attractive boundaries. They found, like Walton et al, that segment-selective surfaces stabilized parallel morphologies and gave thickness-dependent domain orientation, whereas PL was stable for all film thicknesses in the case of neutral walls. Matsen (14) and Tang & Witten (15) also used SCF calculations to examine this system while additionally including the possibility of mixed-orientation or hybrid morphologies that exhibit both surface-parallel and surface-perpendicular components (see, for example, the AHY morphology of Figure 1*c*). While both studies concluded that these mixed forms were metastable only for the case of symmetric boundary conditions and volume symmetric BCs, stable hybrid morphologies were observed in Monte Carlo simulations of similar systems by Kikuchi & Binder (18) (and as discussed below in experiments).

Compositionally asymmetric BCs—those that form spheres, columns, or the gyroid structure in bulk—have garnered less theoretical attention regarding their thin film structure, primarily owing to the extra complexity they pose to analytical treatments and the increased computing power needed to capture the extra dimensionality inherent to these materials. Three studies that consider the cylindrical

morphology under symmetric boundary conditions are notable. An analytical treatment of cylinder orientation in thin films, following the formalism of [Turner (11) and Walton et al (12)] was presented by Suh et al (19). This followed an earlier effort by Turner et al (20) who computed the surface affinities required to impose a cylinder to FL transition in thin films using a Ginzburg-Landau formalism. Most recently, using calculations based on so-called dynamic density functional theory, Huinink et al (21) have produced an extensive analysis of the cylinder morphology that outlines both domain orientation transitions and motif shifts as a function of surface energetics and film thickness. In particular, these researchers found that symmetric boundaries with a strong affinity for the cylinder-forming (minority) BC component could induce formation of FL, which seemingly captures the behavior observed in the experiments of Radzilowski et al (22), discussed below.

EXPERIMENTS Symmetric boundary conditions can be realized experimentally in free-standing films and when films are sandwiched between two substrates. Sandwiched systems were first used by Lambooy et al (23) and Koneripalli et al (24) to probe confinement/surface effects on BC film morphology. In these studies, hard boundaries (evaporated SiO_2 in the former case, glassy polymer in the latter) introduced to the system were strongly attractive to one of the copolymer blocks, a condition that greatly stabilizes surface parallel morphologies (12, 25). Accordingly, each team observed contraction and expansion of the lamellar period as the film thickness was ramped through values incommensurate with multiples of L_0, despite the entropic penalties inherent in these structures. While surface-perpendicular domain orientations in diblock films had been previously seen experimentally (26), Kellogg et al were first to induce lamellar reorientation through symmetric boundary conditions (27). Neutral boundary conditions for polystyrene-b-poly(methyl methacrylate) (PS-b-PMMA) were created by sandwiching this diblock between films of an equimolar random copolymer (RC) of styrene and MMA. This technique was later refined by Huang et al (28–30). Using a better estimate of the RC composition required for surface-energy neutrality in the PS/PMMA system as reported by Mansky and coworkers (31, 32), highly oriented PL (28, 29) and surface-perpendicular cylindrical domains (33) were observed. The innovative techniques these researchers used to localize the RC layers at the BC film surfaces are discussed below. A notable, more quantitative discussion concerning the design of neutral surfaces for a given BC system can be found in Reference 30.

Freestanding films offer the other experimental opportunity to observe symmetric boundary conditions in constrained BC systems. Although the inherent fragility of such films makes examination of these specimens formidable, Radzilowski and coworkers (22), through elegant sample preparation and cross-sectional TEM, tracked the thickness-dependent morphology of cylinder-forming PS-b-poly(butadiene) (PS-b-PB). They noted several trends. Thicker films showed surface-parallel layering, with surfaces composed of half-lamellar layers of PB, despite the entropic expense, as a means of producing the lower surface tension (and here, minority) component at the surface. Karim et al observed this near-surface structure

previously via reflectometry (34). For the thinnest films ($t < L_0$), the consequence of these surface layers is found in an observed change in motif from surface-parallel PB cylinders to volume-asymmetric FL, i.e., thin PB layers sandwiching a PS core. Given the entropic expense associated with this latter morphology, this transition indicates the dominance of surface energetics on the system. As mentioned above, these observations likely find a theoretical framework through the recent calculations of Huinink and coworkers (21). It would be interesting to see these calculations expanded to include asymmetric energetic boundary conditions, discussed next, and thus used to describe substrate-supported films.

Asymmetric Boundary Conditions—Substrate-Supported Films

Although identical film surface boundaries simplify some analyses, many film systems involve asymmetric boundary conditions, i.e., where the block-segment/surface interactions, S_1 and S_2, are different in strength and/or sign. This is certainly the case for substrate-supported films that form the majority of technologically relevant and experimentally tractable specimens. In supported film systems, the surface energy of a given monomer can differ from its substrate interfacial energy by an order of magnitude (25). Furthermore, as discussed below, the presence of asymmetric boundary conditions can result in specific morphological trends—for example, the formation of hybrid morphologies that combine surface-parallel and surface-perpendicular components—that cannot be accounted for with symmetric surface energetics. Accordingly, the understanding of substrate-supported films requires analysis that explicitly includes boundary condition asymmetry.

THEORY Several published studies have employed boundary condition asymmetry in analytical and computational analyses of the morphology of volume-symmetric diblock copolymers. Walton et al (12) included this case in their analysis of lamellar domain orientation and defined conditions for the stability of the PL morphology analogous to that supplied for symmetric boundary conditions. Matson also considered this case using SCF methods (14). This latter work centered generally on film thicknesses greater than L_0. Mixed-orientation morphologies were included in the analysis, making possible predictions comparable to recent observations of such structures by Huang et al (35) in this thickness regime. However, Matson's conclusion was that these hybrid forms are metastable. In contrast, another recent study by Tang (36) considered the case of L_0-thick films under asymmetric boundary conditions. While that work did not consider thickness effects, it succeeded in demonstrating the stability of a particular hybrid morphology (AHY in Figure 1*c*), which had been observed in the PS/PMMA system via transmission electron microscopy (TEM) by Morkved & Jaeger (37) and inferred from reflectivity measurements by Russell et al (38). Tang's study also predicts a number of new morphologies that have yet to be observed.

We recently completed a comprehensive SCF analysis of the morphological behavior of compositionally symmetric, substrate-supported diblock films in the thickness regime $t \leq L_0$ (25). Predicted morphology trends were compared with concurrent experimental observations on a series of PS-b-poly(*n*-alkyl methacrylate) materials supported by silicon substrates. A discussion of our model and main results are presented next.

Two-dimensional SCF calculations were performed using the diblock thin film model of Pickett & Balazs (13). Compositionally symmetric diblock copolymers were modeled on a lattice as chains N statistical segments in length, each segment occupying one lattice space, with an A/B segmental repulsion quantified by the Flory interaction parameter χ_{AB}. Thin films were modeled by confining chains to a rectangular lattice, t units high (x) and $r > t$ units long (y). The substrate boundary (1) at $x = 0$ was energetically selective of the B segments with an interaction energy of S_1^B, whereas the (impenetrable) free surface boundary (2) at $x = t$ was selective of either the B segments (for most of the calculations performed) or the A segments (representing anti-symmetric boundary conditions), but always with an interaction energy (S_2) of lower magnitude than the substrate interaction, i.e., $|S_1| \geq |S_2|$. The conditions $S_1^A = -S_1^B$ and $S_2^A = -S_2^B$ were further imposed to simplify the calculation. Two-dimensional morphologies (analogous to film cross sections) were calculated from a variety of initial conditions (39), and phase diagrams were compiled from graphical and free energy data as described in Reference 25.

The stable morphologies calculated in our study, as summarized in Figure 1*c*, are presented in the general order (with decreasing film thickness) in which they occur and identified by abbreviations defined below. The images shown are cross-sectional views of the calculated film morphologies. The gradients depict the calculated density of B segments. Black indicates 100% B segments, white 100% A segments. In addition to the FL, AFL (anti-symmetric, surface-parallel lamellae) and PL morphologies discussed above, three other film structures are indicated. The HL, or half lamella, is the first ($n = 0$) stable morphology in the classical anti-symmetric thickness series and consists of a half layer of B segments next to the substrate capped by a half layer of A. The HY or hybrid morphology is a mixed-orientation structure consisting of a surface-parallel wetting layer of B at the substrate with surface-perpendicular protrusions approximately $L_0/2$ in width, extending through a half layer of A to the free surface. The HY structure resembles the mixed-orientation lamellar phases predicted by Kikuchi & Binder (18, 40) and by other later studies (14, 15, 36). In contrast to those studies, however, the HY structure is predicted to be a stable morphology for thicknesses below L_0. The AHY, or anti-symmetric hybrid morphology mentioned above with respect to the work of Tang (36), was also found. The relationship between these hybrid forms, HY and AHY, is discussed below.

Figure 2*b* shows these morphologies in the context of an example phase diagram. Here, the ordinate gives the reduced film thickness t/L_0. The abscissa $R = S_2^B/S_1^B$ gives a measure of the asymmetry of the surface energetics. The sign of R distinguishes symmetric (+) and anti-symmetric (−) wetting conditions. The

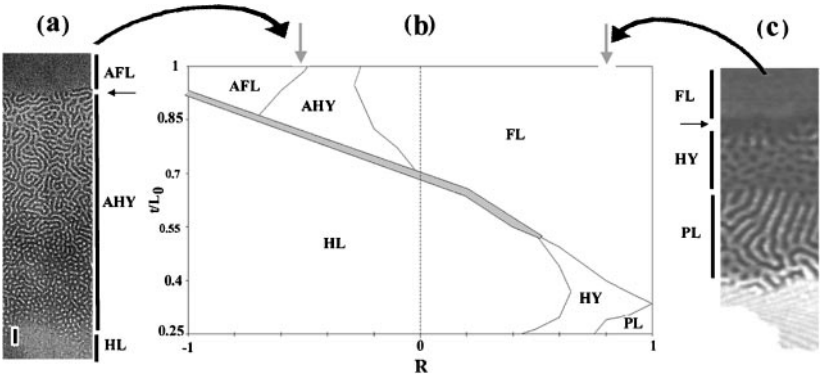

Figure 2 Comparison of predicted morphologies with experimental observations. (*a*) TEM micrograph of anti-symmetric wetting PS-b-PMMA thin film as observed by Morkved et al (reprinted with permission from 37, copyright 1997 EDP Sciences). This film section decreases in thickness from $3/2L_0$ to $1/2L_0$ moving from the top. PS domains appear dark. The morphologies that appear are labeled on the right using abbreviations from Figure 1*c*. The horizontal arrow indicates where a drop in film thickness occurs as described in the text. (*b*) Phase diagram of thin film morphologies calculated with the following parameters: $N = 200$, $S_1^B = -0.3$ kT, $\chi_{AB} = 0.1$. $R = S_2^B/S_1^B$. Phase fields are labeled with abbreviations from Figure 1*c*. The gray area marks where the HY morphology is metastable. Vertical gray arrows (*top*) indicate behavior of PS-b-PMMA (*left*) and PS-b-PLMA (*right*). (*c*) AFM phase micrograph of PS-b-PLMA droplet edge. The film thickness decreases from the top from L_0 to 0. Softer PLMA domains appear dark. Morphologies observed are indicated on the left and the horizontal arrow denotes a sharp drop in film thickness [sections (*b*) and (*c*) are reprinted with permission from 25, copyright 2000 Am. Chem. Soc.].

phase fields are labeled with abbreviations found in Figure 1*c* and designate conditions for which each morphology is predicted to be stable. The hatched area (along the FL/HL border) is a region of HY metastability.

The positive (symmetric wetting) values of R are considered first. For symmetric surface energetics ($R = 1$) a single morphological transition occurs from FL to PL, as other studies have predicted (12, 14, 41). With increasing energetic asymmetry ($0 < R < 1$), the PL phase field splits, giving way first to a region in which the HY structure gains stability, then to another new phase field, the HL morphology. Thus as the surface interactions become more asymmetric, morphologies that lack a horizontal plane of symmetry (i.e., HY and HL) are favored. On the whole, the system behavior can be divided into two regimes based upon the existence of a stable HL phase. For more asymmetric values of R, a stable HL phase intervenes in the transition from FL to the perpendicular structures (HY and PL). As R becomes larger, a direct transition from FL to HY (or PL) occurs.

As seen in Figure 2*b*, the HY phase field is typically situated between the surface parallel morphologies (FL or HL) and the PL phase. With both surface-parallel and surface-perpendicular elements, this structure may be seen as a compromise

morphology that serves as an intermediate between fully parallel and fully perpendicular states. Moreover, the metastable existence of the HY morphology between the FL and HL phase fields suggests that such hybrids are possible intermediates between parallel-symmetric and anti-symmetric morphologies as well. This possibility is pursued further in the discussion of experimental observations (below). A more complete discussion of the effects of the molecular (N, χ_{AB}) and surface-energy (S_1^B) parameters on the morphological behavior of this system can be found in Reference 25.

Different behavior is noted for the anti-symmetric ($R < 0$) portion of the phase diagram. Here, no perpendicular phases are found in the sub-$L_0/2$ thickness region. Indeed, thinner films are all predicted to have the HL morphology, consistent with the classical view of anti-symmetric systems. Overall, three regimes of behavior are observed in our calculations. Generally, these trends are reflected in the morphology of the film near L_0, which is based on the degree of surface-energy asymmetry, i.e., the magnitude of R. This is consistent with the work of Tang (36) whose analysis focused on morphological behavior in this thickness regime. For nearly equal A and B affinities for the surface and substrate, respectively ($R \approx -1$), the AFL morphology is stable, as predicted previously (11, 12, 14). When R is negative but small, there exists a region of FL stability for $t > 0.5L_0$. In this case, the entropic drive toward L_0 periodicity overcomes the penalty of localizing B segments at the S_2 surface. For intermediate values of R, a window of stability appears for the AHY structure. Similarities exist between this morphology and the HY structure found for $R > 0$. First, the AHY appears, like the HY, to be dependent upon boundary condition asymmetry. Also, like the HY, the AHY morphology seems to be an energetic compromise but between surface-parallel states. While our calculations do not extend into the $t > L_0$ thickness regime, the analysis of Matsen (14) strongly indicates that the AHY phase field is bounded above by an anti-symmetric surface-parallel lamellar structure (AFL). Furthermore, the position of the AHY phase field between the AFL and FL indicates its status as intermediary between anti-symmetric and symmetric structures as R is changed. Indeed, the mixed composition of AHY at the free surface (2) surface provides a plausible transition between the B-wetting FL and the A-wetting AFL.

To elaborate further, the AHY may be seen as a fusion of two "half-period" films, each responding to local asymmetric surface energetics. The HL morphology, constituting the bottom half of the film, optimizes S_1^B energetics, as the B block wets the substrate. [This condition was implicit in previous calculations by Tang & Witten (15) who "quenched" this section of film into a static HL morphology.] In the top half of the film, the A segments are favored at both the free surface and at the HL substrate but with differing affinities, now determined by the differential surface energies and the attraction of A for itself. The consequence is the formation of the hybrid morphology, where A segments now form the contiguous surface-perpendicular features. Hence, the HL and HY structures combine to form the AHY morphology.

We see this deconstruction of the AHY structure as interesting in ways that transcend the particulars of anti-symmetric wetting systems. For when considered in this light, the behavior of such films is identical to the symmetric wetting systems, only shifted $0.5L_0$ in thickness. The latter shows a hybrid morphology near $0.5L_0$, whereas the former exhibits these structures near L_0. A conjugate trend is already known to govern the sequence of stable surface-parallel states for each case (6, 10, 42), i.e., symmetric systems exhibit a surface-parallel state at L_0, whereas anti-symmetric systems find these at $0.5L$ and $3/2L_0$. Thus $t < L_0$-thick films are unified under the nL_0 and $(n + 1/2)L_0$ paradigm widely used to describe the morphology of thicker films (6, 10, 42). Framing the question in this manner also suggests that the structure of thin lamellar films can be understood through a general half-period principle of morphological development. Indeed, this half-period principle seemingly applies to the structure of thicker lamellar films also and may well be a way of re-examining between period lateral morphologies as well as explaining hybrid morphologies in more complex copolymer systems as they are observed. Some of these possibilities are considered below in the discussion of experimental observations on substrate-supported systems.

EXPERIMENTS Before continuing, an important difference between real supported films and those considered in the majority of model systems discussed above must be distinguished. Theoretical analyses of thin films most often place the specimen between hard, impenetrable boundaries. Real films supported by simple substrates, however, have only one such boundary. The existence of a free surface (indeed, a form of boundary asymmetry in itself) has important consequences on the film morphology. This can be illustrated by considering a substrate-supported lamellar BC film that exhibits symmetric wetting. Recall that at equilibrium, this system exhibits a series of stable films for $t = nL_0$ ($n = 1, 2, 3, 4 \ldots$). Now, consider the case of an as-cast substrate-supported film of thickness t_i, such that $nL_0 < t_i < (n + 1)L_0$ with ($n \geq 1$), i.e., the film thickness is not commensurate with the equilibrium period of the copolymer. Upon annealing, the morphology of this system develops such that this thickness mismatch with the copolymer periodicity is resolved. This is accomplished by a bifurcation into film regions having two distinct thicknesses, which represent the closest conditions of stability, i.e., nL_0 and $(n+1)L_0$. [Excellent more quantitative illustrations of this phenomenon can be found in the analyses of Matsen (14) and Huinink et al (21).] Accordingly, the free surface forms plateaus, of $(n + 1)L_0$ height on a foundation of film that is nL_0 thick (9, 10). The film area fractions of these quantized domains mirror the degree of mismatch so that the amount of thicker film is almost exactly equal to $t_i/(\mathrm{n} + 1)L_0$, whereas the thinner film fraction is $1-t_i/(n + 1)L_0$. (9) In common nomenclature, when the area of thicker film is less than one half, the higher regions are isolated from each other and are thus called islands. Likewise, isolated lower regions (when the area of thinner film is less than one half) are called holes. In film systems that exhibit a thickness gradient, e.g., the edges of droplets, this effect manifests itself as a series of step-like L_0-high terraces that accommodate the change in

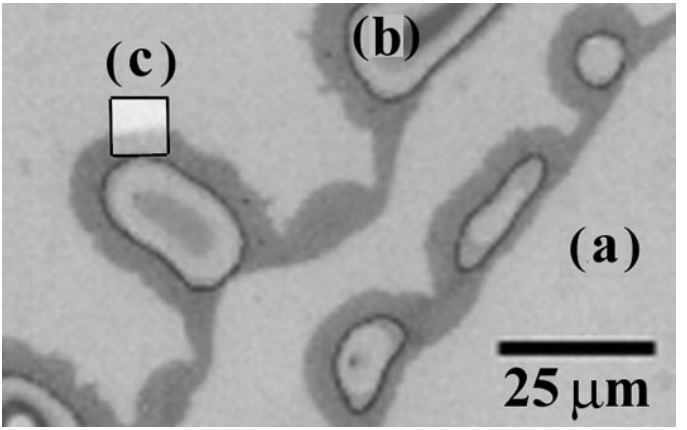

Figure 3 Optical micrograph of lamellar PS-b-PnBMA droplets exhibiting FL morphology and the terracing phenomenon. (*a*) Silicon substrate, (*b*) terraced droplet. Bands of contrast indicate specific optical interference conditions caused by quantized L_0-sized (43 nm) jumps in film thickness. (*c*) Example area (light box) for AFM analysis. An exposed region of bare substrate allows film thickness determination.

thickness. An example of a terraced BC droplet can be seen in Figure 3. In this optical micrograph of a compositionally symmetric PS-b-poly(butyl methacrylate) (PS-b-PBMA) system, the discrete jumps in film thickness are observable because of an optical interference condition with the substrate that selects for the reflection of a specific wavelength of light. Terracing has been most studied for lamellar systems but has been seen for off-symmetric BC compositions as well (22, 43).

Indeed, it was observations of this terracing phenomenon with optical microscopy that led Kämpf and coworkers (7) to first conclude that BC films organize into discrete layers and hypothesize the FL morphology. The verification of this hypothesis, however, came through a series of groundbreaking experiments by Russell and coworkers (6, 38, 42, 44, 45). These researchers probed thin lamellar films with X-ray and neutron reflectivity, demonstrating the ABBA-patterned and L_0-periodic internal structure that characterizes the FL morphology. This same group also established that even when the BC was well above its bulk order/disorder transition temperature, surface effects could induce FL layering (42, 45, 46), as predicted theoretically by Fredrickson (8).

Domain reorientation (formation of PL) owing to thickness constraints were first observed in supported films by Henkee et al (26) through TEM analysis of BC droplet edges. Another study conducted by Carvalho et al (47) showed that terrace edges in ordered BC droplets exhibited surface-perpendicular domains. These edge regions are necessarily incommensurate with L_0, thus demonstrating that intermediate film thicknesses induce lamellar reorientation (12, 14, 25). The authors hypothesized that these perpendicular domains are PL that extend from

the film surface to the substrate. However, in light of the theoretical analysis of supported films presented above, an explanation invoking a topmost-layer HY (or AHY) morphology may be more appropriate.

Mixed-orientation morphologies have also been observed in supported films. Fasolka et al (48) observed the HY morphology in symmetric wetting systems. Morkved & Jaeger (37) first noted the AHY structure [inferred by Russell et al (38)] in anti-symmetric BC films. Thicker ($t > L_0$) films supported by an energetically neutral substrate have also exhibited mixed-orientation lamellae as shown by Huang and coworkers (35).

We have recently completed an extensive empirical study of BC film morphology focusing on the $t < L_0$ thickness regime (25). This work employed a series of lamellar PS-b-poly(*n*-alkyl methacrylate) copolymers supported by silicon substrates with native oxide surfaces. For all but PS-b-PMMA, this homologous series exhibits symmetric wetting (of the methacrylate block) but also offers a range of free-surface and substrate interactions. Hence these systems are comparable to our model calculations described above. A useful AFM (atomic force microscopy) technique facilitated the study of film structure at the edges of ordered BC microdroplets. (In Figure 3, the light box shows a typical area of analysis). These droplet edges exhibit a profile of film thickness from 0 (substrate) to L_0. Simultaneous AFM height and phase imaging of these areas allowed for the concurrent measurement of film thickness (height, when an area of bare substrate is included in the image) and local morphology (phase, which is modulated by elasticity differences between the PS and polymethacrylate domains). Through this technique, accurate correlations between domain orientation and film thickness can be made. Figure 2*c* (*right*) shows a typical AFM phase micrograph collected from an annealed droplet of PS-b-poly(lauryl methacrylate) (PS-b-PLMA). In this image, darker areas are the softer PLMA domains; the brighter areas are PS. The lightest region at the bottom of the image is the substrate. The film thickness ranges from L_0 to 0 going from top to bottom, as noted to the right of the image. Immediately apparent is the thickness-dependent morphological behavior. At L_0, the lack of phase contrast denotes the homogeneous surface layer of the FL morphology. This is followed by a sharp drop in film thickness (arrow), constituting a terrace edge analogous to those discussed above, but with a magnitude of approximately $L_0/2$. All the specimens in the series we examined had this feature. Below the terrace edge, a shelf (approximately $L_0/2$ thick) of film exhibiting a hybrid morphology (labeled HY) is shown. This structure consists of a thin wetting layer of PLMA at the substrate with surface-perpendicular cylindrical (seen as round in plan-view) protrusions extending through the PS layer to the top surface. This is thought to be the three-dimensional equivalent of the two-dimensional hybrid (HY) structure seen in our calculations. (A more detailed discussion of this can be found in Reference 25.) The thinnest regions of film exhibit the PL morphology (Figure 2*c*).

One of the notable things about the behavior of PS-b-PLMA films is that an area of HL is not observed in the $L_0/2$ thickness regime. This is in contrast to e.g., PS-b-PBMA, which shows all of the same morphologies, FL, HY, PL, but

with an additional region of HL between the FL and HY regimes. Although both materials exhibit symmetric wetting of the methacrylate block, the sequence of morphologies as film thickness decreases is different. When morphological data from all of the specimens were considered, they could be classed into two groups, distinguished by the existence of a stable HL phase. Entirely similar to SCF predictions for $R > 0$ in Figure 2*b*, methacrylates with more asymmetric surface/substrate interactions (e.g., ethyl, propyl, and butyl methacrylate) exhibited FL, HL, HY, and PL; those with more symmetric interactions (hexyl, octyl, and lauryl methacrylate) show only FL, HY, and PL (noted by the *right* gray arrow in Figure 2*b*).

Although an equally detailed experimental study of anti-symmetric film morphology does not currently exist, Morkved & Jaeger (37) have examined one system, namely bulk-lamellar PS-b-PMMA. They used TEM to probe films of this material deposited on electron-transparent silicon nitride windows known to be attractive to PMMA. The comparatively lower surface tension of PS favors this block at the free surface. Figure 2*a* shows a micrograph from their study. The section of film shown here decreases in thickness from the top of the image ($t \approx 3/2L_0$) to the bottom ($t \approx L_0/2$). Again, thickness-dependent morphological changes are apparent. The dark band of film with no lateral contrast at the top of the image is the AFL structure. There is a drop in film thickness (indicated with an arrow) of approximately $L_0/2$ to a shelf of film L_0 thick, which exhibits a morphology with a surface-perpendicular component. This is the three-dimensional analogue to the AHY discussed above. Finally, in the thinnest regions at the bottom of the image, contrast disappears, indicating a second surface-parallel form, now HL. This sequence mirrors a cascade of morphologies predicted for anti-symmetric systems, marked by the *left* gray arrow in Figure 2*b*. Note also, as discussed above, how this behavior is similar to that of the symmetric PS-b-PLMA films, only shifted to thicker films by approximately $L_0/2$. This supports the half-period principle of morphological behavior stated above.

SURFACE MORPHOLOGY AND CHEMICAL MOSAICS The conventional view of multicomponent polymer films posits that such systems express a chemically homogeneous surface consisting of the lowest surface tension (γ) constituent. For the most part, the behavior of BC films conforms to this postulate, as exemplified by, e.g., the FL and AFL morphologies. Likewise, systems with an inherent lateral structure, i.e., films of spheres and columns, most often exhibit homogeneous film surfaces even when surface homogeneity poses an entropic penalty, as in cases where the lower surface energy block is in the minority.

However, surface-perpendicular morphologies, such as the HY and PL structures, offer the possibility of film systems with heterogeneous surfaces—nanometer scale chemical mosaics—that could be harnessed as templates in a variety of applications. Our recent SCF analysis of these structures indicates that surface morphology is governed not only by differential surface energetics, but also by the interfacial (χ_{AB}) penalty exacted by so-called capping layers of the low-γ

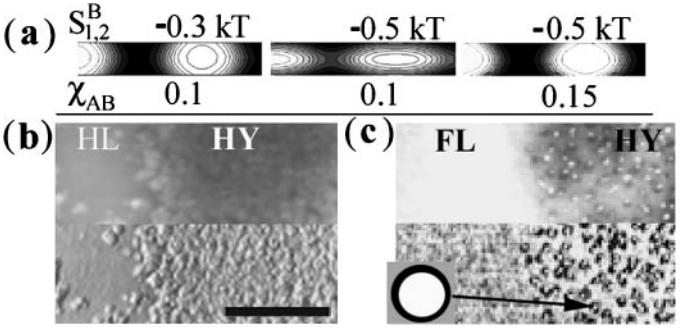

Figure 4 Surface heterogeneity and thin film morphology (49). (*a*) SCF calculations of PL morphology using various surface and interfacial energetics. Static parameters: $N = 200$, $R = 0.9$, $t = L_0/4$. *Left* and *right* bars, heterogeneous surfaces; *middle* bar, homogeneous surface. (*b*) AFM micrograph showing PS-b-PPMA ($\Delta\gamma = 7.4$ dynes/cm, $\chi_{AB} = 0.01$) thin film exhibiting HL and HY morphology, treated with cyanoethylacrylate (CEA) glue vapor. *Upper*: height; *lower*: phase. Polymerized CEA completely covers area with HY indicating a homogeneous PPMA capping layer. (*c*) AFM of PS-b-PLMA ($\Delta\gamma = 7.9$ dynes/cm, $\chi_{AB} = 0.083$) thin film also treated with CEA vapor. *Upper*: height; *lower*: phase. CEA nodules selectively decorate PLMA HY domains indicating a heterogeneous surface. Schematic in phase image shows hard CEA nodule (white) centered on softer PLMA domain. Scale bar indicates 250 nm for (*b*) and (*c*).

component (49). This interplay between surface energy and χ_{AB} is illustrated in Figure 4*a*, which shows the PL morphology calculated under different energetic conditions. Increasing the attraction of B-segments to the surfaces drives this system toward surface homogeneity (Figure 4*a*, *left* and *middle*). However, through a concurrent increase in χ_{AB} (Figure 4*a*, *left* and *middle*), surface heterogeneity is recaptured through the increased A/B interfacial penalty associated with capping.

Experimental observations of such distinctions are difficult because capping layers can be sufficiently thin [only ≈0.5 nm by some reports (50)] to elude reliable detection via X-ray photoelectron spectroscopy or other means. Recently, we adopted a surface-staining technique, developed by forensic scientists to enhance latent fingerprint traces (51, 52), that shows promise in illuminating surface heterogeneity. We treated laterally structured (HY forming) PS-b-PnMA films with cyanoethylacrylate (super glue) monomer vapor (49). The glue monomer preferentially polymerizes (anionically, via ambient H_2O initiation) over the more chemically similar methacrylate domains, forming hard nodules that can be imaged via AFM. These nodules formed a continuous coating over HY morphologies of some of the BC films, as shown for the example of PS-b-poly(propyl methacrylate), PS-b-PPMA, in Figure 4*b*, indicating a homogeneous methacrylate surface. For PS-b-PLMA films, however, the nodules were located specifically over methacrylate domains, as shown in Figure 4*c*, strongly indicating a surface mosaic. Interestingly, the surface energy difference ($\Delta\gamma$), i.e., the driving force toward a homogeneous

surface, is larger for the PS-b-PLMA system than for PS-b-PPMA, as shown in Figure 4. However, PS-b-PLMA has a much higher value of χ_{AB} (see Figure 4) than PS-b-PPMA, making the penalty of a PLMA capping layer comparatively higher, thus resulting in surface heterogeneity for this system. Therefore, it seems that BC chemical mosaic surfaces are a possibility in systems with small $\Delta\gamma$ values and a large χ_{AB}. This suggests, for example, that the PS-b-PMMA system, which fulfills both of these criteria, may also exhibit a heterogeneous surface in its AHY morphology, as previous reports have implied (38, 53).

Developing Trends and Open Arenas

In this section, developing trends in BC thin film research are described, and generally, limited to basic research, i.e., work that more directly contributes to an understanding of the physics of substrate-supported BC film systems in areas not discussed above. Work that takes the field of BC films into new directions is emphasized. In addition, some areas in which little or no research has been completed are outlined.

OFF-SYMMETRIC COMPOSITIONS Most of the published research on BC films concerns bulk-lamellar systems. This is due, in part, to the relative simplicity of the system, in particular the dimensional reduction available to theoretical treatments. However, the inherent three-dimensional nature of the off-symmetric motifs—gyroid, cylinders and spheres—provides extra degrees of freedom for consideration and, further, make these forms interesting for certain technological applications, e.g., lithographic masks (54, 55). This is not to say that the extensive research effort invested into lamellar systems has no bearing on these systems. Rather, many of the tenets outlined above for compositionally symmetric BC films (e.g., a general surface-parallel domain orientation, the effect of the neutrality condition, etc) can and have been applied to systems of off-symmetric composition. However, some aspects of these thin film systems, in particular the consequences of their inherent interfacial curvature, probably cannot be fully understood without thorough experimentation and direct theoretical focus.

Of the other BC motifs, the cylindrical morphology has received the most attention. Basic experimental studies on confinement effects and domain orientation in substrate-supported cylinder-forming diblock films were first performed by Henkee et al (26) using TEM. Since then, studies have been published by Liu et al (56), Karim et al (34), and Harrison et al (43, 57, 58) among others (59–61). Of these, the work of Harrision et al (43, 57) is particularly noteworthy, in part because of the elegant imaging technique they used for studying these systems. A layer-by-layer scanning electron microscopy (SEM) method gave three-dimensional morphological information superior to the surface-localized imaging of AFM used in References 56, 59, 60, and TEM images (26), which become confusing if more than a monolayer of structure is present. By alternating a nonselective etching process with low-voltage SEM it is possible to track morphological behavior through

the film from the free surface, achieving domain contrast through conventional OsO_4 staining. This method revealed detailed images of domain orientation, terrace edge defects, and novel morphologies, including hybrid forms. As in earlier studies (34), Harrison et al noted that for cylinder systems in which the minority component has a lower surface energy, the near-surface regime is composed of a planar wetting layer. This surface effect was also seen (see above) in freestanding films (22).

Theoretical descriptions of cylinder-forming films are sparse. This is unfortunate, because an adequate theoretical framework would help organize the various, sometimes conflicting, observations noted in the literature. Of the few efforts completed (19, 20), the work of Huinink et al (21), discussed above, stands apart for its ability to depict complex and observed phenomena in this system (22). However, as stated before, the symmetric boundary conditions used by these researchers, while an excellent foundation, are inadequate for describing substrate-supported films. An expanded theory might address some basic concerns regarding films of bulk-cylindrical diblocks. Liu and associates (56), for example, have noted that the persistence of surface-parallel layering in cylindrical systems is quite limited, compared with that in films of lamellar and spherical systems, which are known to maintain such layering for film thicknesses many times L_0.

Supported bulk-spherical BC film systems, despite their promise as nanoscopic lithographic masks, have been the subject of very few publications. To date, there does not seem to be a theoretical treatment of spherical thin film morphology. Experimental studies, for the most part, are geared toward simple observations of structure (26), imaging techniques (57), or device applications (55). Two recent efforts by Yokoyama and coworkers (62, 63), however, include detailed physical insight into the spherical phase in supported thin films. Using secondary mass ion spectrometry (SIMS) and AFM, they have probed both the through-film and lateral structure of this system under a variety of conditions, examining the effects of molecular weight, film thickness, and annealing time/temperature on film structure and surface topography (island and hole formation). An interested theorist would do well to address these findings.

Of the gyroid phase in thin films, almost nothing has been published. One experimental piece by Chan et al (64) deals with this film system, but the work is primarily directed toward technological applications. The gyroid morphology offers a unique symmetry and interconnected structure, and it would be interesting to know the conditions under which BCs exhibiting such a morphology maintain this structure as thin films. Given its (compositional) position between lamellae and cylinders in the classical BC phase diagram, the opportunity to observe surface-induced motif shifts from gyroid to these bordering forms seems likely.

LIQUID-CRYSTALLINE AND SEMI-CRYSTALLINE BC FILMS While we have hitherto considered amorphous materials, the inclusion of non-amorphous components into block copolymer molecules is not uncommon, and an understanding of their bulk behavior is fairly well established (see citations in References 65 and 66).

Research into liquid crystalline (LC) and semi-crystalline BC thin films, however, has only very recently begun.

One promise of BCs with an LC component (most systems still have one amorphous block) is the ability to alter and control morphology (of both LC and BC) through an interplay between the L_0-periodic BC microphase separation and the finer periodicity of LC ordering. Thin film geometries add surface energy considerations and confinement effects, now on two levels of periodicity, to this equation. The first observations of such complexity were by Wong and coworkers (65) who compared films of PS-b-LC (smectic) diblocks with symmetric and off-symmetric compositions. The symmetric material was found to exhibit a PL structure with smectic layering parallel to the surfaces in the LC domains. The asymmetric system was found to form FL with surface-perpendicular smectic layers. A later work by Sentenac et al (67) investigated the bulk and thin film behavior of a compositionally asymmetric PS-b-LC diblock with LC as the minority component. The films showed a novel morphology that exhibited both FL and a surface-parallel smectic phase. Finally, Hammond and coworkers (68) have recently studied thin films of volume-symmetric diblocks incorporating a side chain-LC block, in the $t < 2L_0$ thickness regime. They found a film structure exhibiting both a mixed-orientation morphology (an effect, it seems, of surface energy asymmetry) and an interesting surface topography that included terracing on both the L_0 and smectic length scales. Theoretical treatments (currently there are none) that explicitly include thin film effects on each level of order could greatly enhance our understanding of such systems.

Like LC-containing systems, BCs with a semi-crystalline component also offer an additional length scale of competing order manifest in the periodicity of the crystalline phase. In addition, the morphology of these systems is a strong function of the thermal history imparted through processing (69). The final microstructure these materials adopt depends upon whether microphase separation or crystallization occurs first. A few studies have considered this competition in BC thin films (66, 70–72). For example, in studying PS-b-poly(ethylene) (PS-b-PE), De Rosa et al (72) observed a variety of interesting and useful path-dependent structures, including surface-perpendicular crystalline PE cylinders and highly aligned PL. A similar effect was noted by these researchers (66) for triblock copolymers with PE end-blocks and an amorphous poly(ethylene)/poly(propylene) mid-block. This work and reorientation trends observed by Reiter et al (70) are described in more detail below.

BC BLENDS AND BC/HOMOPOLYMER BLENDS Blending block copolymers with other BCs or homopolymers can alter the morphology of the system in interesting ways. It is well known, for example, that addition of homopolymer A to an A-b-B diblock can cause a motif shift in bulk systems because the homopolymer associates with the chemically similar block (73). BC/BC blends have also shown intriguing microphase and dual-microphase behavior in bulk (50, 74). Furthermore, recent predictions by Leibler et al (75) propose that diblock/triblock blends

could result in non-centro-symmetric morphologies that would have a variety of interesting physical and optical properties.

Thin film diblock/diblock blends were first explored by Mayes et al (76), who studied bimodal mixtures of long- and short-volume-symmetric PS-b-PMMA materials supported by silicon substrates. Using deuterated short chains and neutron reflectivity, these researchers found that for a range of compositions, the smaller diblocks localized at the PS/PMMA interfaces of larger FL structures. This is interesting because it opens the possibility of creating structures with localized functionality within the larger BC morphology. This study additionally demonstrated that the periodicity of such bimodal blends was the same as a unimodal diblock with an equivalent number-averaged molecular weight, as seen in bulk studies (74). Self-consistent field calculations have been used to model similar systems by Shi & Noolandi (77) and others (78), with similar results. Koneripalli et al (78) additionally examined supported diblock/diblock blend films of compositionally asymmetric PS-b-poly(vinyl pyridine) (PS-b-PVP) materials. These researchers found that if the final blend composition was volume-symmetric, the films formed the FL morphology even if the individual diblock constituents exhibited other motifs. Their study included concurrent SCF calculations that showed qualitative agreement with their experimental work.

A few studies of diblock/homopolymer blend thin film behavior are of note. Russell and coworkers (79) examined the PS-b-PMMA/PMMA and PS-b-PMMA/PS blend systems. Using deuterated homopolymers and neutron reflectometry, they probed the effect of homopolymer chain length on its ultimate distribution within the corresponding copolymer domains. When the homopolymer molecular weight was comparable to that of the corresponding block of the copolymer, the chains were accommodated in the center of the block domain (i.e., between the block "brushes"), leading to a period expansion. In contrast, shorter homopolymers were distributed more evenly throughout the block domain, resulting in little or no expansion. Qualitatively similar behavior was noted from SCF calculations of diblock/homopolymer blends by Shull and coworkers (80, 81). More recently, Green and coworkers (82, 83) reached similar conclusions employing AFM to study homopolymer N-dependence on the period (inferred through terrace heights) of PS-b-PMMA/PS and PS-b-PMMA/tetramethylbisphenol A polycarbonate (TMPC) blends, where TMPC exhibits favorable interactions with PS.

Each of the above blend studies focuses on films that are much thicker than L_0. An interesting route for future studies would be to consider film thicknesses that conflict with one or more of the natural length scales in the blend system. In the case of long/short diblock blends, for example, interesting behavior may develop in films when $t < L_0$ for the longer system but is still thick enough to accommodate the shorter component. Analogous work could be completed for diblock/homopolymer blends. Indeed, for very high–molecular weight homopolymers blended into diblocks, early studies made the surprising conclusion that macrophase separation is inhibited by confinement (84). This hypothesis has yet to be fully explored.

TRIBLOCK COPOLYMERS Adding a third block to the copolymer sequence brings added complexity to the thin film picture, especially in the case of A-B-C (versus A-B-A) forms. Indeed, the bulk state phase diagrams for amorphous A-B-C materials is only partially mapped to date, with reports of new morphologies appearing nearly every year (2, 85). While published studies of A-B-A triblock films (86–90) report qualitatively similar behavior to that described above for diblocks, the many specific morphological details that arise out of the inherent combinatorial complexity of A-B-C systems (91–94) make these reports hard to organize into a succinct narrative. This is especially true because an extensive theoretical framework for these systems does not exist. Only one study by Pickett & Balazs (92) considers the system from a theoretical standpoint. These researchers outline the energetics of lamellar domain orientation in A-B-C triblock films using SCF calculations. They find, for example, that if the film surfaces repulse blocks A and C, but are neutral or attractive to the central B block, the PL morphology is stabilized. These findings might be useful in explaining some recent observations, e.g., those of Stocker (91, 93) who reports PL in PS-b-PB-b-PMMA films.

A practical difficulty arises in imaging thin film surfaces of A-B-C triblock materials because the surface chemistry does not necessarily reflect the true system composition, which can make the species identification of morphological domains a challenge. To overcome this obstacle, Elbs and coworkers (94) describe a novel sample preparation technique, applied to PS-b-PVP-b-poly(tert butyl methacrylate) films, in which specimens were briefly exposed to solvent vapors carefully chosen to selectively swell a given block component. The surface reorganization that develops is apparently permanent if drying is accomplished quickly, thereby highlighting the locations of specific block domains under subsequent AFM analysis.

A volume-imaging AFM technique similar to the SEM technique of Harrison et al (57) was demonstrated on a PS-PB-PS film by Konrad and coworkers (89). Using alternating steps of AFM analysis and nonselective plasma etching, film morphology was tracked from the surface through the film, exploiting elasticity differences between PS and PB in phase imaging. A generic A-B-C system would most likely prove more problematic for this method. However, a combination of this technique and the solvent vapor treatment reported by Elbs et al could be useful for these more complex systems.

APPLICATIONS

The possible technological application of block copolymer thin films has been widely recognized. The length scale of microphase separation, 10–100 nm, is particularly interesting to technologists eager to develop a new generation of submicron scale electronic and optical devices. Such schemes would harness the spontaneous self-assembly of these materials to create nanoscopic device components or templates with which such components could be manufactured. Indeed,

by tuning molecular parameters (N, composition, species), microphase domains with a variety of motifs, chemistries, and tailored size and periodicity might be created. Furthermore, recent developments in block copolymer synthesis, such as atom transfer radical polymerization (95), have greatly widened the spectrum of available copolymer materials or decreased their cost of manufacture.

Masks and Membranes

A prime example of a BC thin film application is their demonstrated utility as lithographic masks. In this scheme, ordered (and oriented) layers of microphase domains, deposited onto a suitable substrate, are selectively etched, via a plasma, ozone, or wet chemical means, to remove one of the block components. Holes in the resulting mask can then be used to transfer the BC motif pattern, via other etching or deposition steps, onto the substrate. This was demonstrated first by Mansky et al (96), employing a monolayer of hexagonally ordered diblock spheres. Indeed, the density of features that can be imparted to the substrate in this manner is staggering. Park et al (55), for example, reported 10^{11} etched-features/cm^2 in their refinement of this technique, also accomplished with thin films of sphere-forming diblocks. This system has since been combined with other microfabrication techniques to create equally dense arrays of metal dots (97) and GaAs nanocrystals (98). This same idea of selective etching of BC film domains has also shown potential for the formation of nanoporous membranes, as demonstrated recently by Liu and coworkers (99). In such an application cross-linking of the residual (unetched) matrix can make it stable enough for use, as shown by Nardin et al (90), who produced stable, freestanding, L_0-thick (10 nm) membranes with areas in excess of 1 mm^2 from A-B-A triblocks.

BC/Inorganic Composites

The idea of harnessing of BC morphology as a means of creating ultra-fine ordered dispersions of inorganic particles is well established (100). Several research initiatives have recently demonstrated that BCs can be used to create and/or distribute nanometer-sized, metallic (101, 102), magnetic (100, 103, 104), and ceramic (64, 105–109) structures. A plethora of devices, such as terabit-level memory storage media, become possible if the organization of the diblock domains that house these particles can be adequately controlled.

Three general strategies for patterning nanoscopic particulates in BC thin films have been explored: Surface decoration techniques involve the preferential segregation of deposited material to favored domains on a pre-oriented BC film surface (53, 110). In solution-blended composites, bare or surface-activated nano-particles are combined with BC in solution. During film processing, these particles sequester into preferred block domains (111, 112). A theoretical treatment of this phenomenon was published recently by Balazs and coworkers (113). Finally, so-called nanoreactors use inorganic precursors, such as metal salts, engineered to preferentially associate with one component of a BC. This can be accomplished by actually

incorporating the precursor moieties as pendant groups on one of the block species in the system (100, 101), but BC/precursor blends have also been demonstrated to work (114–116). After films are cast and microphase separation occurs, the precursor molecules, now confined to one of the patterned domains, are reduced (or otherwise transformed) in situ to form particles. Later, the polymer may be removed, leaving a nano-patterned inorganic phase on the substrate (64, 115). Figure 5 illustrates a recent result from Leppert and coworkers, who employed sphere-forming PS-b-P4VP films to create periodic arrays of GaN nanoclusters (117).

Long-Range Order, Domain Orientation, and Designed Patterns

The above machinations for incorporating BC films into nanoscopic devices show promise. However, for many applications, technical challenges to these schemes are apparent. First and foremost is the issue of long-range order. Short-range ordering of microphase-separated BC films is excellent (as demonstrated in many published micrographs), but these films also typically exhibit the rich array of defects and grain structure seen in bulk systems. If BC films are to be used as templates in addressable memory applications, one of two conditions must be met: either long-range order needs to be greatly improved (indeed, perfected!) or more robust addressing schemes must be engineered. Furthermore, although the feature size and density offered by the first lithographic masks employing a monolayer of diblock spheres are impressive (55, 118), the aspect ratio of sharp features prepared

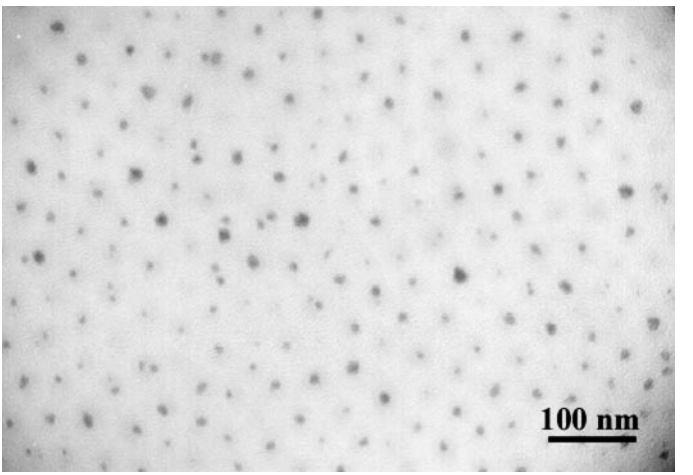

Figure 5 TEM image of film of PS-b-Poly(4-vinyl pyridine) doped with gallane-trimethylamine and processed to form a nanoparticle array. GaN nanoparticles are sequestered to spherical poly(4-vinyl pyridine) domains of the microphase-separated copolymer. Micrograph courtesy of Leppert (117).

by such ultra-thin masks is limited to about 1. If deeper features are to be created, the use of thicker films may be necessary, as might be accomplished, for example, with surface-perpendicular cylinder formations. Thus techniques to induce and control BC domain orientation in substrate-supported films remain important. Finally, the types of patterns natural BC films offer remain limited to the spatial motifs (spheres, columns etc) determined by thermodynamics. Widening the scope of self-assembly in film systems to include designed patterns would increase the usefulness of BC films. Several research efforts have explored strategies for surmounting one or more of these challenges, as discussed below.

ENGINEERING SURFACE EFFECTS The orientation of domains in block copolymer films is highly dependent upon the surface energy boundary conditions imposed on the system. In particular, surface fields that are neutral with respect to each of the blocks induce the formation of surface-perpendicular microphase domains (12). This effect has been exploited by Huang et al to impart a surface-perpendicular orientation in both lamellar and cylindrical PS-b-PMMA systems (28–30). Neutral surfaces were fabricated from PS/PMMA random copolymers (RCs) (27) of carefully tuned composition (30–32), localized at the film surfaces through the following means. At the substrate, RC chains of appropriate composition were end-grafted to the surface, forming a dense brush that could not diffuse into the cast diblock film. Additional RC chains of the same composition were end-functionalized with short poly(tetrafluoroethylene) (PTFE) segments. When incorporated into the diblock film, these RCs self-assembled at the free surface owing to their low surface energy chain ends, thereby creating a neutrality condition. Figure 6*a* shows a cylinder-forming DBC film specimen processed in this manner (33). Well-oriented cylindrical domains on a roughly hexagonal lattice are seen in this AFM micrograph. Demonstrations of the usefulness of these oriented films as lithographic masks and templates were recently published (33). Energetically neutral surfaces that induce domain orientations have also been reported by Peters et al (119), who chemically modified octadecyltrichlorosilane self-assembled monolayers with X-rays, thus demonstrating that the wetting properties of these layers can be tuned via the X-ray dosage.

In an effort to understand and control grain-boundary defect formation, movement, and elimination in diblock films with in-plane periodicity, Harrison et al (57, 58) studied such defects in specimens of cylinder- and sphere-forming systems, using the layer-by-layer SEM method described above. To examine the effect of surface interactions on defects and the degree of order, monolayer PS-b-PB films of surface-parallel cylinders (PB) were compared for two different substrate conditions: a bare silicon substrate and a substrate modified with an end-grafted PS brush (58). They found a lower defect density and greater persistence length for films with the brush-modified substrate, which they attributed to the reduced interaction strength between PB domains and the substrate. Strong substrate interactions can immobilize or pin defects, leaving them unable to participate in the processes by which these features collect and are eliminated.

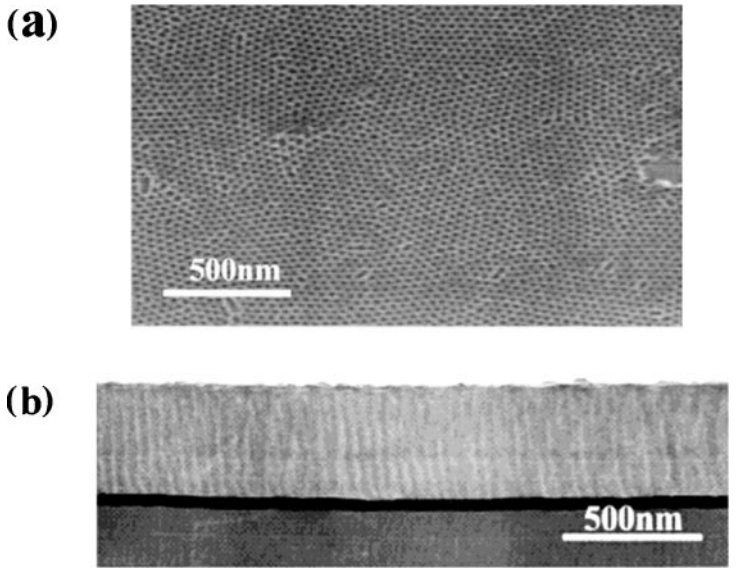

Figure 6 Oriented cylinders in diblock films. (*a*) Plan-view FESEM micrograph of PS-b-PMMA cylinders oriented perpendicular to the substrate plane via neutral surface energetics (28, 33). In this image, the PMMA phase has been preferentially etched away. Note the in-plane grain structure. (*b*) Cross-sectional TEM micrograph of PS-b-PMMA cylinders oriented by application of a through-film electric field (33). The film lies atop the dark band, an Au electrode layer, and shows surface-perpendicular cylinders that bridge the free and substrate surfaces. (reproduced with permission from 33, copyright 2000 Wiley & Sons, Inc).

APPLICATION OF EXTERNAL FIELDS Following bulk studies by Amundson and coworkers (120, 121), Morkved et al (122) examined the effect of an applied electric field on BC thin film morphology. Microfabricated electrodes were applied the E-field in the plane of the film during annealing. The resulting morphology exhibited in-plane cylinders oriented perpendicular to the electrode faces, i.e., aligned parallel to the E-field lines. Hence, as illustrated by Thurn-Albrecht et al (33, 123), application of the field perpendicular to the film plane induces cylinders into a surface-perpendicular morphology. A micrograph from their study is shown in Figure 6*b*. These researchers (123) have analyzed this situation theoretically as well and propose that the mechanism for alignment is found in the differential polarizability between the block components. Through these calculations, supported qualitatively by experiments by the same group (123), predictions regarding the critical field strength required to overcome the interfacial barriers to cylinder reorientation can be made. One advantage the E-field technique offers to microfabrication (in particular, as discussed above, for lithographic masks) is the thickness of films (up to 1 μm) that can be oriented (33). Indeed, very recently, researchers (124)

have selectively etched E-field oriented films and deposited ferromagnetic cobalt material into the resulting cylindrical holes—a step toward block copolymer-based fabrication of terabit density memory storage media.

Given the success of E-field alignment and the general success of mechanical fields in inducing domain alignment (125) in bulk systems, it is surprising that the application of other fields to BC films has not been attempted. While magnetic fields would not be expected to affect pure BC materials, those doped with magnetic nanoparticles might respond amenably. Temperature gradients successfully used by Bodycomb and coworkers (126) to make millimeter thick single-crystal lamellar BC domains might also prove promising. It would be interesting to see the effect of in-plane temperature gradients on the long-range order of laterally organized BC film morphologies such as spheres and columns.

PATTERNED SUBSTRATES Substrates imparted with chemical and/or topographic patterns offer means of directing microphase separation in BC films. By using such substrates, local domain orientation, film surface morphology, and long-range order can be affected and sometimes controlled. In addition, substrate patterns can widen the scope of microphase domain structure beyond those motifs offered by nature.

Diblock films deposited onto chemically heterogeneous surfaces have recently received substantial attention. Recent years have seen a flood of publications reporting theoretical treatments of diblock films on chemically patterned substrates, led by the groundbreaking work of Balazs and coworkers (127–137). Generally, these studies discerned the effect of the substrate pattern periodicity on film morphology. In particular, when the period of the substrate pattern approaches molecular dimensions, these studies predict (almost universally) a surface-perpendicular orientation of the block domains.

This promise of morphological control dictates that experimental studies of diblock films on chemically patterned surfaces be pursued. Facilitated by the emergence of microcontact printing techniques (138), Heier et al (139–141) examined the effect of micron-scale substrate chemical heterogeneity on bulk-lamellar diblock films. This team demonstrated that contrasting wetting symmetries across patterned substrates induces a surface pattern of islands and holes that mirrors the substrate periodicity (140). They have used this effect to study the kinetics of island formation and coarsening (141). An X-ray lithography technique (134) recently allowed Yang and coworkers (142) to examine similar effects on the submicron scale.

Rockford et al (143) published the first observations of diblock films (compositionally symmetric PS-b-PMMA) on heterogeneous substrates with nanoscopic periodicity. The substrates they fabricated and employed had alternating stripes of gold and silicon, selectively attractive to PS and PMMA, respectively. They found that the PL morphology formed when the copolymer and pattern periods matched. Moreover, the only defects in this perpendicular morphology were due to flaws in the substrate pattern itself. When the substrate period was longer or shorter than L_0, diblock recognition of the underlying pattern was diminished. Similar

observations were reported by Yang and coworkers (142) on surfaces produced by their lithographic technique.

Patterned substrate topography offers another means of manipulating BC film morphology. Li et al (144) examined symmetric BC films on micron-scale corrugated substrates. Interestingly, they found that islands were formed preferentially over the corrugation troughs, creating a surface that was anti-conformal with the substrate undulations. Moreover, this resulted in terrace-edge defects aligned perpendicular to the substrate corrugations. We have also studied the effect of surface topography on diblock films and demonstrated a lateral patterning technique based on the thickness dependence of film morphology and domain orientation (25, 48). This originally employed faceted silicon substrates (145) exhibiting sawtooth-profile corrugations of ∼2-nm amplitude and periods in the 100-nm range. Thin films of PS-b-PBMA deposited on these substrates exhibited a flat free surface, in accordance with predictions by Turner & Joanny (146). This implies a periodic film thickness profile: thinner above corrugation peaks, thicker above troughs. Accordingly, if the average film thickness is chosen correctly, i.e., such that these thickness modulations occur about a critical thickness at which a morphological transition takes place, a lateral domain pattern develops that mirrors the substrate topography, as demonstrated in the micrograph in Figure 7*a*. Here the diblock film is, on average, about $L_0/3$ (∼15 nm) thick. Near this film thickness, the HY morphology gives way to PL. The corrugated substrate (∼210-nm period) laterally modulates the film thickness such that HY (dots) are formed over the troughs whereas the thinner morphology, PL, is formed on the peaks. As a result, a complex lateral patterning with a unique motif develops, as shown. A dual-scale (nanometer, micron) pattern can develop if micron-sized features are used, as in Figure 7*b*. In this case the film surface is nearly conformal over the 30-nm high, 1.5-μm wide substrate columns. However, the film thins slightly as it bends over the column edges. Choosing the film thickness to be just below $L_0/2$, where the HL to HY transition occurs, results in the preferential formation of HY (dots) on the edges of the substrate features. Thus through the use of substrate topography, diverse film patterns with a range of length scales can be created. This patterning technique has motivated a recent theoretical treatment by Podariu & Chakrabarti (147). These researchers compare HY formation on flat and corrugated substrates, demonstrating, as we previously observed (48) and discuss above, that these features preferentially form over topographic peaks and edges where the film is thinner.

CRYSTALLIZATION The path-dependent morphological behavior of semi-crystalline BCs can be exploited to create films with oriented domains and long-range order. Reiter and coworkers (70) demonstrated this behavior with lamellar PB-b-poly(ethylene oxide) (PB-b-PEO). Films of this material were spin cast onto substrates and annealed to induce formation of FL. Cooling leads to crystallization of the PEO within the layered microphase domains. Depending upon the temperature at which the PEO crystallized, various morphologies developed, including, for low temperatures, a highly oriented PL morphology. This reorientation was

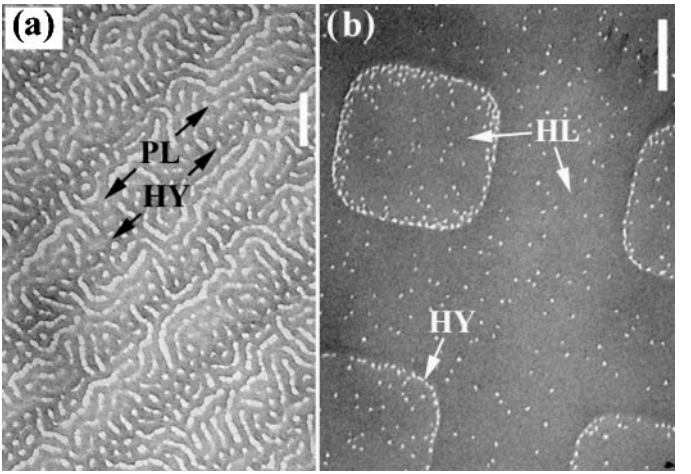

Figure 7 Patterning of DBC films via substrate topography (48). (*a*) TEM micrograph of PS-b-PBMA film peeled (25) from corrugated substrate with 210-nm period. PS domains appear dark. Thickness effects cause alternating HY and PL morphologies to form over corrugation troughs and peaks, respectively. Scale bar = 200 nm. (*b*) Dual-scale pattern of HY morphology. TEM micrograph of PS-b-PBMA film deposited on 30-nm high silicon posts with 1.5-mm diameter and 4-mm spacing. The HY morphology forms preferentially where the film is thinnest at the edges of the post. Areas without contrast are the HL morphology. Scale bar = 1 μm.

conjectured to accommodate the volume change that accompanies crystallization. De Rosa et al (66, 72) also examined crystallization-induced domain orientation. The key to their technique was the use of a crystallizable solvent (benzoic acid) into which the semi-crystalline PS-b-PE was dissolved. Directional solidification of the solvent between two glass plates led to well-oriented crystals of this small molecule that act as a template onto which the polymer crystallizes epitaxially (indeed, this might be considered a patterned surface technique!). Dependent upon BC composition, arrays of surface-perpendicular cylinders or PL were observed, both exhibiting good long-range order. The authors further noted the speed of this technique and its applicability to large-area films.

Optical Properties—Future Development of BC Films as Photonic Devices

It is well known that planar multi-layered dielectric systems exhibit useful optical properties, as evidenced by the widespread use of various band pass and notch optical filters. These "one-dimensional photonic crystals" selectively reflect a certain wavelength of light owing to their periodic structure and Fabry-Perot interference effects (148). The reflected wavelength (position of the optical band gap) is

directly related to the layer periodicity and the dielectric contrast, i.e., the difference in the index of refraction between the component materials in the layered system. Indeed, if designed correctly, as demonstrated recently by Fink and coworkers (149), the band gaps of alternating multilayered systems shed their angular dependence. Such omnidirectional dielectric reflectors can serve as peerless wave guides capable of directing light though near hairpin turns without loss.

The self-assembled morphologies of BC systems make them intriguing candidates for photonic applications. This is especially true of BC film systems that spontaneously exhibit well-defined alternating layered structures. Fink et al (150) have succinctly outlined the materials parameters involved in transforming BC systems into effective photonic materials. Of these, two are most important: First, common BC systems exhibit L_0 values in the 10–100-nm range, whereas photonically active systems require periodicities of hundreds of nanometers. However, ultra-high molecular weight BCs are currently synthesizable, if not yet routine, and, as we have seen (79), increasing the period of FL layers is possible through the addition of homopolymer. In thick film systems, Urbas and coworkers (151, 152) recently proved the efficacy of this concept. Through the addition of two homopolymers (one of each block species), they increased the L_0 of a lamellar-forming diblock into the photonic regime, also demonstrating that the position of the band gap could be tuned through the amount of added homopolymer. These authors found, however, that defects in the lamellar structure were problematic. It appears that the increased order offered by approaches described above would be of benefit. The second barrier to block copolymer photonic activity is dielectric contrast. Most polymer systems have nearly identical indices of refraction. Nevertheless, this can be altered, as discussed above, by the selective doping of microphase domains with high index particles (111, 149, 150).

The real promise BC thin films offer to photonics applications might be found in their in-plane ordering. Here, laterally distributed domains would exhibit an in-plane two-dimensional optical band structure that could be harnessed in a variety of ways (148, 150). For such applications, control of domain order, orientation, and pattern are required. The means for such control are available, as described above. The question is whether they can be applied to higher-L_0 systems, which are known to pose a significant kinetic challenge. Another challenge will be in characterizing in-plane photonic film structures as they are being developed. While various spectroscopic techniques provide an ensemble picture of photonic activity, essential information about these systems will be found in the optical activity of small groups of microphase domains and single defects. The size of these structures places them beyond the reach of conventional far-field optical microscopies. Fortunately, the recent emergence of near-field scanning optical microscopy (NSOM) offers the opportunity to image structures below the diffraction limit with light (see 153 for a review of this technique). Indeed, NSOM has been established as a tool for probing the local optical structure of inorganic two-dimensional photonic crystals (154, 155), and initial examinations of photonic BC films are currently underway (156).

SUMMARY AND CONCLUSIONS

The behavior of BC films is rooted in a balance between surface energetics, which find increased importance in film systems, and confinement effects, i.e., conflicts between the equilibrium period of microphase separation, L_0, and the film thickness. In even the simplest situations, compositionally symmetric diblocks under symmetric surface energetics, these governing principles are the source of a rich array of morphological behavior. Indeed, the prevalence of surface-parallel domain layering, the thickness dependence of domain orientation, and the reorientation effect of surface neutrality can be witnessed under symmetric boundary conditions. However, some phenomena, in particular those associated with substrate-supported films, require a consideration of surface energy asymmetry, i.e., different segmental affinities for the substrate and free surfaces. When these effects are included, a more comprehensive picture of diblock film behavior develops. Hybrid morphologies, which include both surface parallel and surface perpendicular components, seem to be a direct consequence of boundary asymmetry. Moreover, through this more complete picture, an organizing principle of morphology, based around $L_0/2$-thick units, can be outlined for lamellar film systems that unites the symmetric and anti-symmetric wetting regimes and structures observed over a range of thickness. Such a principle may lend insight when examining more complex systems such as asymmetric BC compositions, chemistries including crystalline and liquid crystalline components, and A-B-C triblock copolymers, discussed above.

Recent research efforts have suggested the utility of thin BC films as components in a new generation of optical and electronic devices. Lithographic and microfabrication techniques using BC films offer unprecedented feature dimensions and densities. Moreover, elegant methods of harnessing their microphase separation to produce fine, ordered dispersions of inorganic material are in development. However, for many potential applications, e.g., addressable memory devices, limitations arise from the imperfect long-range order and restricted choice of motifs. Headway has been made through exploitation of surface and confinement effects, application of external fields, and use of chemically and topographically patterned substrates. These approaches for morphological control evolved directly from research on the fundamental physics of block copolymer films. Thus understanding the physics of block copolymer film structure remains a worthwhile pursuit.

ACKNOWLEDGMENTS

This work was supported primarily by the MRSEC program of the National Science Foundation under Award DMR-98-08941. MJF thanks the Research Associateship Program of the National Research Council. The authors thank Dr. Valerie Leppert for providing the micrograph in Figure 5.

LITERATURE CITED

1. Bates FS, Fredrickson GH. 1990. *Annu. Rev. Phys. Chem.* 41:525
2. Thomas EL, Lescanec RL. 1994. *Philos. Trans. R. Soc. London Ser. A* 348:149
3. Matsen MW. 1998. *Curr. Opin. Colloid Interface Sci.* 3:40
4. Gido SP, Gunther J, Thomas EL, Hoffman D. 1993. *Macromolecules* 26:4506
5. Gido SP, Thomas EL. 1994. *Macromolecules* 27:849
6. Russell TP, Coulon G, Deline VR, Miller DC. 1989. *Macromolecules* 22:4600
7. Kämpf G, Hoffmann M, Krömer H. 1970. *Ber. Bunsenges. Phys. Chem.* 71: 851
8. Fredrickson GH. 1987. *Macromolecules* 20:2535
9. Coulon G, Collin B, Ausserre D, Chatenay D, Russell TP. 1990. *J. Phys.* 51:2801
10. Ausserre D, Chatenay D, Coulon G, Collin B. 1990. *J. Phys.* 51:2571
11. Turner MS. 1992. *Phys. Rev. Lett.* 69: 1788
12. Walton DG, Kellogg GJ, Mayes AM, Lambooy P, Russell TP. 1994. *Macromolecules* 27:6225
13. Pickett GT, Balazs AC. 1997. *Macromolecules* 30:3097
14. Matsen MW. 1997. *J. Chem. Phys.* 106:7781
15. Tang WH, Witten TA. 1998. *Macromolecules* 31:3130
16. Geisinger T, Muller M, Binder K. 1999. *J. Chem. Phys.* 111:5241
17. Geisinger T, Muller M, Binder K. 1999. *J. Chem. Phys.* 111:5251
18. Kikuchi M, Binder K. 1994. *J. Chem. Phys.* 101:3367
19. Suh KY, Kim YS, Lee HH. 1998. *J. Chem. Phys.* 108:1253
20. Turner MS, Rubinstein M, Marques CM. 1994. *Macromolecules* 27:4986
21. Huinink HP, Brokken-Zijp JCM, van Dijk MA, Sevink GJA. 2000. *J. Chem. Phys.* 112:2452
22. Radzilowski LH, Carvalho BL, Thomas EL. 1996. *J. Polym. Sci. B* 34:3081
23. Lambooy P, Russell TP, Kellogg GJ, Mayes AM, Gallagher PD, Satija SK. 1994. *Phys. Rev. Lett.* 76:2899
24. Koneripalli N, Singh N, Levicky R, Bates FS, Gallagher PD, Satija SK. 1995. *Macromolecules* 28:2897
25. Fasolka MJ, Banerjee P, Mayes AM, Pickett G, Balazs AC. 2000. *Macromolecules* 33:5702
26. Henkee CS, Thomas EL, Fetters LJ. 1988. *J. Mater. Sci.* 23:1685
27. Kellogg GJ, Walton DG, Mayes AM, Lambooy P, Russell TP, et al. 1996. *Phys. Rev. Lett.* 76:2503
28. Huang E, Rockford L, Russell TP, Hawker CJ. 1998. *Nature* 395:757
29. Huang E, Russell TP, Harrison C, Chaikin PM, Register RA, et al. 1998. *Macromolecules* 31:7641
30. Huang E, Pruzinsky S, Russell TP, Mays J, Hawker CJ. 1999. *Macromolecules* 32:5299
31. Mansky P, Liu Y, Huang E, Russell TP, Hawker C. 1997. *Science* 275:1458
32. Mansky P, Russell TP, Hawker CJ, Mays J, Cook DC, Satija SK. 1997. *Phys. Rev. Lett.* 79:237
33. Thurn-Albrecht T, Steiner R, DeRouchey J, Stafford CM, Huang E, et al. 2000. *Adv. Mater.* 12:787
34. Karim A, Singh N, Sikka M, Bates FS, Dozier WD, Felcher GP. 1994. *J. Chem. Phys.* 100:1620
35. Huang E, Mansky P, Russell TP, Harrison C, Chaikin PM, et al. 2000. *Macromolecules* 33:80
36. Tang WH. 2000. *Macromolecules* 33:1370
37. Morkved TL, Jaeger HM. 1997. *Europhys. Lett.* 40:643

38. Russell TP, Menelle A, Anastasiadis SH, Satija SK, Majkrzak CF. 1991. *Macromolecules* 24:6263
39. Scheutjens JMHM, Fleer GJ. 1979. *J. Phys. Chem.* 83:1619
40. Kikuchi M, Binder K. 1993. *Europhys. Lett.* 21:427
41. Pickett GT, Witten TA, Nagel SR. 1993. *Macromolecules* 26:3194
42. Anastasiadis SH, Russell TP, Satija SK, Majkrzak CF. 1989. *Phys. Rev. Lett.* 62:1852
43. Harrison C, Park M, Chaikin P, Register RA, Adamson DH, Yao N. 1998. *Macromolecules* 31:2185
44. Russell TP, Menelle A, Anastasiadis SH, Satija SK, Majkrzak CF. 1992. *Makromol. Chem.-Macromol. Symp.* 62:157
45. Anastasiadis SH, Russell TP, Satija SK, Majkrzak CF. 1990. *J. Chem. Phys.* 92:5677
46. Menelle A, Russell TP, Anastasiadis SH, Satija SK, Majkrzak CF. 1992. *Phys. Rev. Lett.* 68:67
47. Carvalho BL, Thomas EL. 1994. *Phys. Rev. Lett.* 73:3321
48. Fasolka MJ, Harris DJ, Mayes AM, Yoon M, Mochrie SGJ. 1997. *Phys. Rev. Lett.* 79:3018
49. Fasolka MJ. 2000. PhD thesis. *The morphology and lateral patterning of diblock copolymer thin films.* MIT, Cambridge, MA. 174 pp.
50. Hasegawa H, Hashimoto T. 1992. *Polymer* 33:475
51. Kendall FG, Rehn BW. 1983. *J. Forensic Sci.* 28:777
52. Kobus HJ, Warrener RN, Stoilovic M. 1983. *Forensic Sci. Int.* 23:233
53. Zehner RW, Lopes WA, Morkved TL, Jaeger H, Sita LR. 1998. *Langmuir* 14:241
54. Mansky P, Chaikin PM, Thomas EL. 1995. *J. Mater. Sci.* 30:1987
55. Park M, Harrison C, Chaikin PM, Register RA, Adamson DH. 1997. *Science* 276:1401
56. Liu Y, Zhao W, Zheng X, King A, Singh A, et al. 1994. *Macromolecules* 27:4000
57. Harrison C, Park M, Chaikin PM, Register RA, Adamson DH, Yao N. 1998. *Polymer* 39:2733
58. Harrison C, Chaikin PM, Huse DA, Register RA, Adamson DH, et al. 2000. *Macromolecules* 33:857
59. Nick L, Lippitz A, Unger W, Kindermann A, Fuhrmann J. 1995. *Langmuir* 11:1912
60. Vandijk MA, Vandenborg R. 1995. *Macromolecules* 28:6773
61. Hahm J, Sibener SJ. 2000. *Langmuir* 16:4766
62. Yokoyama H, Mates TE, Kramer EJ. 2000. *Macromolecules* 33:1888
63. Yokoyama H, Kramer EJ, Rafailovich MH, Sokolov J, Schwarz SA. 1998. *Macromolecules* 31:8826
64. Chan VZH, Hoffman J, Lee VY, Iatrou H, Avgeropoulos A, et al. 1999. *Science* 286:1716
65. Wong GCL, Commandeur J, Fischer H, de Jeu WH. 1996. *Phys. Rev. Lett.* 77:5221
66. De Rosa C, Park C, Lotz B, Wittmann JC, Fetters LJ, Thomas EL. 2000. *Macromolecules* 33:4871
67. Sentenac D, Demirel AL, Lub J, de Jeu WH. 1999. *Macromolecules* 32:3235
68. Wu JS, Fasolka MJ, Hammond PT. 2000. *Macromolecules* 33:1108
69. Cohen RE, Cheng PL, Douzinas K, Kofinas P, Berney CV. 1990. *Macromolecules* 23:324
70. Reiter G, Castelein G, Hoerner P, Riess G, Blumen A, Sommer JU. 1999. *Phys. Rev. Lett.* 83:3844
71. Lammertink RGH, Hempenius MA, Vancso GJ. 2000. *Langmuir* 16:6245
72. De Rosa C, Park C, Thomas EL, Lotz B. 2000. *Nature* 405:433
73. Winey KI, Thomas EL, Fetters LJ. 1991. *Macromolecules* 24:6182
74. Hashimoto T, Yamasaki K, Koizumi S, Hasegawa H. 1993. *Macromolecules* 26:2895
75. Leibler L, Gay C, Erukhimovich I. 1999. *Europhys. Lett.* 46:549
76. Mayes AM, Russell TP, Deline VR, Satija

SK, Majkrzak CF. 1994. *Macromolecules* 27:7447
77. Shi AC, Noolandi J. 1994. *Macromolecules* 27:2936
78. Koneripalli N, Levicky R, Bates FS, Matsen MW, Satija SK, et al. 1998. *Macromolecules* 31:3498
79. Mayes AM, Russell TP, Satija SK, Majkrzak CF. 1992. *Macromolecules* 25: 6523
80. Shull KR, Winey KI. 1992. *Macromolecules* 25:2637
81. Shull KR, Mayes AM, Russell TP. 1993. *Macromolecules* 26:3929
82. Orso KA, Green PF. 1999. *Macromolecules* 32:1087
83. Smith MD, Green PF, Saunders R. 1999. *Macromolecules* 32:8392
84. Pan T, Huang KL, Balazs AC, Kunz MS, Mayes AM, Russell TP. 1993. *Macromolecules* 26:2860
85. Brinkmann S, Stadler R, Thomas EL. 1998. *Macromolecules* 31:6566
86. Vandenberg R, deGroot H, Vandijk MA, Denley DR. 1994. *Polymer* 35:5778
87. Kim G, Libera M. 1998. *Macromolecules* 31:2569
88. O'Connor SM, Gehrke SH, Retzinger GS. 1999. *Langmuir* 15:2580
89. Konrad M, Knoll A, Krausch G, Magerle R. 2000. *Macromolecules* 33:5518
90. Nardin C, Winterhalter M, Meier W. 2000. *Langmuir* 16:7708
91. Stocker W, Beckmann J, Stadler R, Rabe JP. 1996. *Macromolecules* 29:7502
92. Pickett GT, Balazs AC. 1998. *Macromol. Theory Simul.* 7:249
93. Stocker W. 1998. *Macromolecules* 31: 5536
94. Elbs H, Fukunaga K, Stadler R, Sauer G, Magerle R, Krausch G. 1999. *Macromolecules* 32:1204
95. Matyjaszewski K. 1999. *Macromol. Symp.* 143:257
96. Mansky P, Harrison CK, Chaikin PM, Register RA, Yao N. 1996. *Appl. Phys. Lett.* 68:2586
97. Park M, Adamson DH, Chaikin PM, Register RA. 1999. In *ACS PMSE Proc.* 81:12–13
98. Li RR, Dapkus PD, Thompson ME, Jeong WG, Harrison C, et al. 2000. *Appl. Phys. Lett.* 76:1689
99. Liu GJ, Ding JF, Hashimoto T, Kimishima K, Winnik FM, Nigam S. 1999. *Chem. Mater.* 11:2233
100. Ciebien JF, Clay RT, Sohn BH, Cohen RE. 1998. *New J. Chem.* 22:685
101. Chan YNC, Craig GSW, Schrock RR, Cohen RE. 1992. *Chem. Mater.* 4:885
102. Ciebien JF, Cohen RE, Duran A. 1998. *Supramol. Sci.* 5:31
103. Sohn BH, Cohen RE. 1997. *Chem. Mater.* 9:264
104. Sohn BH, Cohen RE, Papaefthymiou GC. 1998. *J. Magn. Magn. Mater.* 182:216
105. Sankaran V, Cummins CC, Schrock RR, Cohen RE, Silbey RJ. 1990. *J. Am. Chem. Soc.* 112:6858
106. Cummins CC, Schrock RR, Cohen RE. 1992. *Chem. Mater.* 4:27
107. Kane RS, Cohen RE, Silbey R. 1999. *Chem. Mater.* 11:90
108. Kane RS, Cohen RE, Silbey R. 1999. *Langmuir* 15:39
109. Lee T, Yao N, Aksay IA. 1997. *Langmuir* 13:3866
110. Morkved TL, Wiltzius P, Jaeger HM, Grier DG, Witten TA. 1994. *Appl. Phys. Lett.* 64:422
111. Mattoussi H, Radzilowski LH, Dabbousi BO, Fogg DE, Schrock RR, et al. 1999. *J. Appl. Phys.* 86:4390
112. Limary R, Swinnea S, Green PF. 2000. *Macromolecules* 33:5227
113. Ginzburg VV, Gibbons C, Qiu F, Peng GW, Balazs AC. 2000. *Macromolecules* 33:6140
114. Spatz JP, Roescher A, Moller M. 1996. *Adv. Mater.* 8:337
115. Spatz JP, Mossmer S, Hartmann C, Moller M, Herzog T, et al. 2000. *Langmuir* 16:407
116. Eibeck P, Spatz JP, Mossmer S, Moller M,

Herzog T, Ziemann P. 1999. *Nanostruct. Mater.* 12:383
117. Leppert VJ, Risbud SH, Stender M, Power PP, Banerjee P, et al. 2000. *J. Am. Chem. Soc.* In review
118. Harrison C, Park M, Chaikin PM, Register RA, Adamson DH. 1998. *J. Vac. Sci. Technol. B* 16:544
119. Peters RD, Yang XM, Kim TK, Sohn BH, Nealey PF. 2000. *Langmuir* 16:4625
120. Amundson K, Helfand E, Davis DD, Quan X, Patel SS, Smith SD. 1991. *Macromolecules* 24:6546
121. Amundson K, Helfand E, Quan XN, Hudson SD, Smith SD. 1994. *Macromolecules* 27:6559
122. Morkved TL, Lu M, Urbas AM, Ehrichs EE, Jaeger HM, et al. 1996. *Science* 273:931
123. Thurn-Albrecht T, DeRouchey J, Russell TP, Jaeger HM. 2000. *Macromolecules* 33:3250
124. Thurn-Albrecht T, Schotter J, Kästle GA, Emley N, Tuominen MT, et al. 2000. *Science* 290:2126
125. Hamley IW. 1998. *The Physics of Block Copolymers*. Oxford, UK: Oxford Univ. Press
126. Bodycomb J, Funaki Y, Kimishima K, Hashimoto T. 1999. *Macromolecules* 32:2075
127. Huang KL, Balazs AC. 1991. *Phys. Rev. Lett.* 66:620
128. Balazs AC, Gempe MC, Zhou ZX. 1991. *Macromolecules* 24:4918
129. Balazs AC, Huang KL, McElwain P, Brady JE. 1991. *Macromolecules* 24:714
130. Chakrabarti A, Chen H. 1998. *J. Polym. Sci. B* 36:3127
131. Petera D, Muthukumar M. 1998. *J. Chem. Phys.* 109:5101
132. Wang Q, Nath SK, Graham MD, Nealey PF, de Pablo JJ. 2000. *J. Chem. Phys.* 112:9996
133. Wang Q, Yan QL, Nealey PF, de Pablo JJ. 2000. *Macromolecules* 33:4512
134. Yang XM, Peters RD, Kim TK, Nealey PF. 1999. *J. Vac. Sci. Technol. B* 17:3203
135. Chen H, Chakrabarti A. 1998. *J. Chem. Phys.* 108:6897
136. Pereira GG, Williams DRM. 1998. *Phys. Rev. Lett.* 80:2849
137. Pereira GG, Williams DRM. 1999. *Langmuir* 15:2125
138. Kumar A, Whitesides GM. 1993. *Appl. Phys. Lett.* 63:2002
139. Heier J, Kramer EJ, Walheim S, Krausch G. 1997. *Macromolecules* 30:6610
140. Heier J, Genzer J, Kramer EJ, Bates FS, Walheim S, Krausch G. 1999. *J. Chem. Phys.* 111:11101
141. Heier J, Kramer EJ, Groenewold J, Fredrickson GH. 2000. *Macromolecules* 33:6060
142. Yang XM, Peters RD, Nealey PF. 2000. *Macromolecules* 33:9575
143. Rockford L, Liu Y, Mansky P, Russell TP, Yoon M, Mochrie SGJ. 1999. *Phys. Rev. Lett.* 82:2602
144. Li Z, Qu S, Rafailovich MH, Sokolov J, Tolan M, Turner MS, et al. 1997. *Macromolecules* 30:8410
145. Mochrie SGJ, Song S, Yoon MR, Abernathy DL, Stephenson GB. 1996. *Physica B* 221:105
146. Turner MS, Joanny JF. 1992. *Macromolecules* 25:6681
147. Podariu I, Chakrabarti A. 2000. *J. Chem. Phys.* 113:6423
148. Jannopoulos JD, Mead R, Winn JN. 1995. *Photonic Crystals, Molding the Flow of Light*. Princeton, NJ: Princeton Univ. Press
149. Fink Y, Winn JN, Fan SH, Chen CP, Michel J, et al. 1998. *Science* 282:1679
150. Fink Y, Urbas AM, Bawendi MG, Joannopoulos JD, Thomas EL. 1999. *J. Lightwave Technol.* 17:1963
151. Urbas A, Fink Y, Thomas EL. 1999. *Macromolecules* 32:4748
152. Urbas A, Sharp R, Fink Y, Thomas EL, Xenidou M, Fetters LJ. 2000. *Adv. Mater.* 12:812
153. Dunn RC. 1999. *Chem. Rev.* 99:2891

154. McDaniel EB, Hsu JWP, Goldner LS, Tonucci RJ, Shirley EL, Bryant GW. 1997. *Phys. Rev. B* 55:10878
155. Bryant GW, Shirley EL, Goldner LS, McDaniel EB, Hsu JWP, Tonucci RJ. 1998. *Phys. Rev. B* 58:2131
156. Fasolka MJ, Hwang J, Goldner LS, Urbas A, DeRege P, Thomas EL. 2001. *Near-field optical images of photonic block copolymer morphology*. Presented at Gordon Res. Conf.: Polymers. Ventura, CA

Annual Review of Materials Research
Volume 31, 2001

CONTENTS